



Review

# Review of the Simulators Used in Pharmacology Education and Statistical Models When Creating the Simulators

Toshiaki Ara <sup>1,\*</sup>  and Hiroyuki Kitamura <sup>2</sup>

<sup>1</sup> Department of Pharmacology, Matsumoto Dental University, 1780 Gobara Hirooka, Shiojiri 399-0781, Nagano, Japan

<sup>2</sup> Matsumoto Dental University Hospital, 1780 Gobara Hirooka, Shiojiri 399-0781, Nagano, Japan

\* Correspondence: toshiaki.ara@mdu.ac.jp; Tel.: +81-263-51-2102

**Abstract:** Animal experiments have long been used as an educational tool in pharmacological education; however, from the perspective of animal welfare, it is necessary to decrease the number of animals used. Although using of simulators is effective, the development of these simulators is necessary when there is no existing simulator for animal experiments. In this review, we describe free, downloadable, and commercial simulators that are currently used in pharmacological education. Furthermore, we introduce two strategies to create simulators of animal experiments: (1) bioassay, and (2) experiments that measure the reaction time. We also describe five sigmoid curves (logistic curve, cumulative distribution function [CDF] of normal distribution, Gompertz curve, von Bertalanffy curve, and CDF of Weibull curve) to fit the results and their inverse functions. Using this strategy, it is possible to create a simulator that calculates the reaction time following drug administration. Moreover, we introduce a statistical model for local anesthetic agents using hierarchical Bayesian modeling. Considering the correlation among estimated parameters, we suggest it is possible to create simulators that give results more similar to those of animal experiments. The pharmacological education will be possible by these simulators at educational institutions where animal experiments are difficult due to various restrictions. It is expected that the number of simulator-based education programs will increase in the future.

**Keywords:** pharmacological education; animal use alternative; simulator; statistical model; sigmoid curve



Academic Editor: Robert Henry

Received: 7 December 2024

Revised: 20 January 2025

Accepted: 21 January 2025

Published: 24 January 2025

**Citation:** Ara, T.; Kitamura, H. Review of the Simulators Used in Pharmacology Education and Statistical Models When Creating the Simulators. *Appl. Biosci.* **2025**, *4*, 6. <https://doi.org/10.3390/applbiosci4010006>

**Copyright:** © 2025 by the authors. Licensee MDPI, Basel, Switzerland. This article is an open access article distributed under the terms and conditions of the Creative Commons Attribution (CC BY) license (<https://creativecommons.org/licenses/by/4.0/>).

## 1. Introduction

Currently, animal experiments are performed as part of pharmacological education to understand the effects of drugs. Representative drugs include general anesthetic agents (inhalation and intravenous anesthetics), local anesthetic agents, muscle relaxants, autonomic nervous system drugs (sympathetic and parasympathetic nervous system), antiinflammatory drugs, analgesics, hemostatic drugs, and anticoagulants (Table 1). Bioassay is performed to calculate effective dose 50% (ED<sub>50</sub>), toxic dose 50% (TD<sub>50</sub>), and lethal dose 50% (LD<sub>50</sub>) from the presence or absence of a reaction to the drug. Pharmacokinetic experiments are performed by measuring the blood concentration of administered reagents.

**Table 1.** Examples of animal experiments in pharmacological education.

Drugs/Experiments	Measurements	Animals
General anesthetic agent inhalation anesthetics intravenous anesthetics	induction time and duration	mouse
Local anesthetic agents *	blink reflex to stimulation of cornea by hair reaction to stimulation by needle	rabbit guinea pig
Muscle relaxants *	contraction and relaxation of rectus abdominis	frog
Autonomic nervous system drugs *	contraction and relaxation of intestinal tract Magnus method	guinea pig
Antiinflammatory drugs	edema of footpad induced by carrageenin dye leakage from blood vessels in the ear	rat rabbit
Analgesics	reaction to stimulation hot plate test/tail flick test writhing method/formalin method tail pinch method	mouse mouse mouse
Hemostatic drugs anticoagulants	time until bleeding stops from cut tail similar to Duke method	mouse
Bioassay effective dose 50% (ED <sub>50</sub> ) toxic dose 50% (TD <sub>50</sub> )	effect of analgesics convulsions induced by pentetorazol or lidocaine	mouse mouse
Pharmacokinetics *	blood concentration of administrated reagent	mouse/rat

\* Astarisk means that simulators exist in these experiments (see Tables 2 and 3).

As animal welfare becomes increasingly important, a corresponding decrease in the number of animals used for experiments is desirable. In identifying animal alternatives, the 3Rs are an effective strategy: Replacement (directly replace or avoid the use of animals), Reduction (obtain comparable information levels from fewer animals), and Refinement (minimize or eliminate animals' pain and distress, improving their welfare) [1]. From this perspective, the usage of simulators is preferable. However, there are little simulators for pharmacological education. Although several existing simulators are summarized in Tables 2 and 3, the simulators do not exist for most other animal experiments. Therefore, it is desirable to develop new simulators to reduce the number of animals.

**Table 2.** Free downloadable simulators in pharmacological education.

Simulator	Contents
OBSim [2]	organ bath simulator effect of mainly autonomic nervous drugs on intestinal tract
Virtual Cat [2]	simulator of anaesthetized cat effect of drugs on cardiovascular and skeletal muscle systems
RatCVS [2]	simulator of normal and pithed rat effect of drugs on cardiovascular system
Virtual Twitch [2]	simulator of rat phrenic nerve-hemidiaphragm preparation effect of neuromuscular blocking and reversal agents
Virtual NMJ [2]	simulator of electrical potentials at the skeletal neuromuscular junction effect of various drugs effect of changes to ionic composition of the extracellular solution
Virtual Nerve [2]	simulator of action potential firing of a neuron within a brain slice effect of anti-epileptic drugs

**Table 3.** Commercial simulators in pharmacological education.

Simulator	Contents
Pharmacology-PICOS [3]	web-based simulator for pharmacodynamics intestinal motility and blood pressure
BMP-VR (Japanese only) [4]	virtual reality simulator of drug-administrated mice acetaminophen, buprenorphine, diazepam, loxoprofen, morphine, phenobarbital, phenytoin, rocuronium
Simcyp™ [5]	physiologically based pharmacokinetics
PKPlus™ Module extends GastroPlus® [6]	compartment and non-compartment analysis

In this review, we (1) introduce the simulators used in pharmacological education; (2) review statistical models used for creating simulators when there is no existing simulator, with a focus on the curves employed in fitting data; and (3) demonstrate the statistical model and the results by computer simulation based on our recent studies [7,8].

The pharmacological education will be possible by these simulators at educational institutions where animal experiments are difficult due to various restrictions. If these simulators are used in a variety of educational institutions, it is expected that the number of simulator-based education will increase in the future.

## 2. Simulators Used in Pharmacology Education

In this section, we introduce several simulators for animal experiments. In previous studies, Ezeala introduced several free downloadable simulators for teaching pharmacology [9], and Andrews and Barta reviewed several simulators used in clinical pharmacology [10].

### 2.1. Free Downloadable Simulators

As an alternative to animal use, computer simulations are employed in various fields, including organ bath systems, cardiovascular systems (such as Strathclyde Pharmacology Simulations package) [2], and pharmacokinetics [11]. Table 2 summarizes commonly used simulators that are available for free download. The following information is based on the information on each simulator's website and according to the previous study by Ezeala [9].

The Organ-bath Simulator (OBSim) program [2] simulates a classical, *in vitro*, pharmacological experiment using one of four different types of tissue: guinea pig ileum, rabbit jejunum, chick biventer cervicis, and rat artery. OBSim was also used to characterize the pharmacological properties of unknown drugs using guinea pig ileum. Students used the program to determine whether drugs were agonists or antagonists [9].

Virtual Cat [2] is a simulation tool designed to replicate an anesthetized cat experiment, representing a whole animal preparation. It is commonly used to screen the effects of pharmaceutical compounds on the cardiovascular and skeletal muscle systems. Virtual Cat displays the effects of 15 standard drugs and 17 unknown drugs on blood pressure, heart rate, skeletal muscle, and nictitating membrane contractions. Students used the program to investigate the effects of agonists, antagonists, and vasodilators on cardiovascular function [9].

Rat Cardiovascular System, also known as RatCVS [2], is a simulation of a normal and pithed rat experimental preparation for investigating the actions of 22 standard drugs and 10 unknown drugs on the cardiovascular system. Using these systems, tutors provided guidelines according to which the students made inquiries and provided scientific explanations for the observations [9].

Virtual Twitch [2] is a simulation of a rat phrenic nerve-hemidiaphragm preparation. It is used to study the actions of neuromuscular blocking and reversal agents, and other drugs that affect neuromuscular transmission.

Virtual NMJ [2] is a simulation of an experiment recording the electrical potentials associated with neuromuscular transmission at the skeletal neuromuscular junction. The simulation allows students to observe the muscle action potential (AP) and endplate potentials (EPPs) evoked by either nerve stimulation or direct current stimulation of the muscle fiber. The effects of a variety of drugs and of changes to ionic composition of the extracellular solution on AP and EPPs can be studied.

Virtual Nerve, formerly known as EPSim or Rat Brain Slice Epilepsy Simulation [2], is a simulated experiment for investigating the effects of anti-epileptic drugs on the AP firing of a neuron within a brain slice. The intracellular membrane potential of the neuron is recorded using a patch clamp amplifier via a glass micropipette electrode attached to the cell body of the neuron and connected to an oscilloscope recording device. The neuron can also be stimulated via this route. Drugs can be applied to the bath and the concentration of the Na, Ca, and K ions in the bathing medium changed.

Recently, we reported models based on the results of animal experiments for a local anesthetic simulator [7,8]. In these animal experiments, several local anesthetic agents are injected subcutaneously into the shaved backs of guinea pigs, and the number of reactions when stimulated with a needle were measured. Moreover, we created a simulator to use in pharmacology education based on this statistical model [12]. This has succeeded in reducing the number of experimental animals used.

## 2.2. Commercial Simulators

In this section, we will introduce several commercial simulators (summarized in Table 3). The representative simulators are Pharmaco-PICOS [3], BMP-VR [4], Simcyp™ [5], and PKPlus™ Module extends GastroPlus® [6]. The following information is based on the information on each product's website.

The Pharmacological Practice of Intestine and Cardiovascular Organ Simulator (Pharmaco-PICOS) [3] is a web-based simulator for pharmacodynamics. Pharmaco-PICOS simulates the physiological responses observed in the atrium and ileum when they are stimulated with biologically active substances and various therapeutic drugs. In addition, Pharmaco-PICOS simulates the alternation of blood pressure. In the ileum simulator, papaverine, serotonin, ondansetron, chlorpheniramine, and mosapride can be used. In the blood pressure simulator, noradrenaline, phenylephrine, angiotensin II, and losartan can be used.

The Basic Medicine Practice-Virtual Reality (BMP-VR) [4] is a simulator that incorporates VR. Using VR goggles, students can observe the response of mice administered drugs such as acetaminophen, buprenorphine, diazepam, loxoprofen, morphine, phenobarbital, phenytoin, and rocuronium. At present, BMP-VR only supports the Japanese language.

Simcyp™ [5] is a simulator for physiologically based pharmacokinetics. Simcyp™ accurately predicts drug behavior within the human body, aiding in various stages of drug development. Simcyp™ is used to determine optimal dosing for first-in-human trials, optimize clinical study designs, evaluate new drug formulations, predict drug-drug interactions, and conduct virtual bioequivalence analyses. Simcyp™ incorporates extensive libraries on demographics, developmental physiology, and drug elimination pathways, as well as advanced mechanistic organ models and compound files.

PKPlus™ Module extends GastroPlus™ [6] is used to rapidly estimate pharmacokinetic parameters for noncompartmental analysis, as well as 1-, 2-, and 3-compartment PK models from pharmacokinetic studies involving intravenous injection (IV) and/or oral administration. The fitted parameters include PK properties, first order absorption

rate, bioavailability, and absorption lag time. Compartmental PK models can be fitted to individual IV or oral data, as well as to multiple plasma concentration versus time profiles.

### 3. Statistical Models for Computer Simulation

In the following section, we describe the strategy for applying statistical models to experiments where simulators do not exist. To perform a computer simulation, a process is required in which random numbers are used to obtain results based on the statistical models. Simulators are then created using these statistical models.

The animal experiments are divided into at least two categories based on the type of reaction: (1) those that measure the presence or absence of a reaction to drugs, and (2) those that measure reaction time to drugs or changes in body size over time.

Bioassay is an example of the former type (Table 1). In bioassay,  $ED_{50}$ ,  $TD_{50}$ , and  $LD_{50}$  are calculated based on reaction rates at various doses. In this case, two parameters are estimated using probit regression analysis. Using these two parameters, a computer simulation can be performed (Figure 1B).

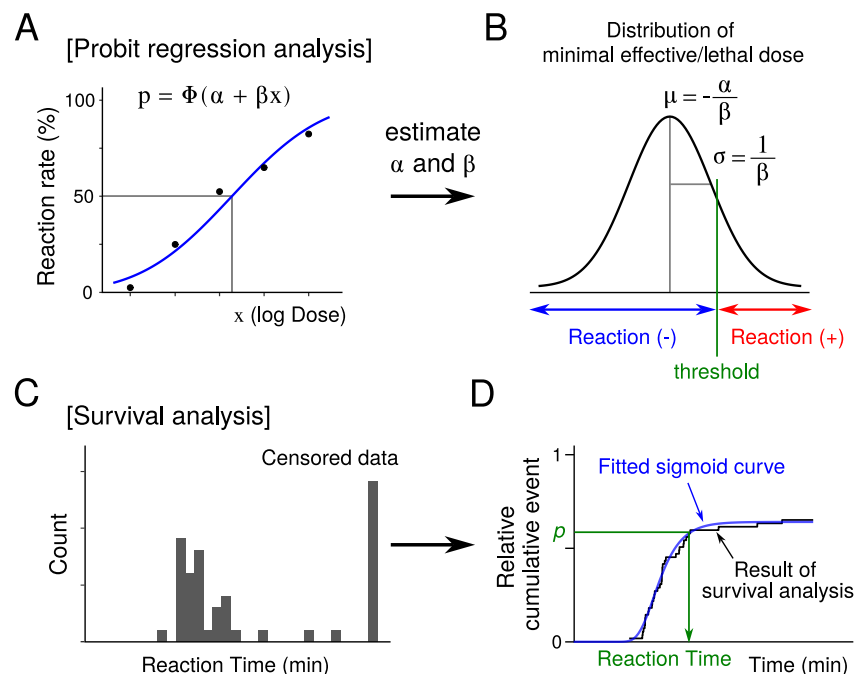


**Figure 1.** Strategies and statistical models for computer simulation. (A,B) Bioassay to estimate effective dose 50% ( $ED_{50}$ ) or lethal dose 50% ( $LD_{50}$ ): Cumulative distribution function (CDF) of normal distribution is fitted to reaction rate ( $p$ ) (A).  $x$  is logarithm of dose, and  $\Phi$  is CDF of normal distribution. The parameters (intercept [ $\alpha$ ] and slope [ $\beta$ ]) are estimated by probit regression analysis. Using these parameters, the distribution of minimal effective/lethal dose is determined. The mean ( $\mu$ ) and standard deviation ( $\sigma$ ) of this distribution are calculated as  $-\alpha/\beta$  and  $1/\beta$ , respectively [solve following simultaneous equations:  $\alpha + \beta\mu = 0$  and  $\alpha + \beta(\mu + \sigma) = 1$ ]. In the computer simulation, minimal effective/lethal dose (threshold) is set using a random number that follows this normal distribution. The presence or absence of a reaction is determined by comparison between the administrated dose and this threshold (B). (C,D) Experiments measuring reaction time from drug administration: The histogram of reaction times. When no reaction was observed within the measurement period, the data were treated as censored (C). The determination of reaction time in the computer simulation: The relative cumulative event is calculated by survival analysis (black line). A sigmoid curve (blue line) is fitted to this result. In the computer simulation, using the inverse function of this sigmoid curve, reaction time is determined from the random number ( $p$ ) that follows to uniform distribution between 0 to 1 (green line) (D).

The latter examples involve several experiments, such as those involving general anesthetic agents (induction time and duration), as well as hemostatic drugs and anticoagulants (time until bleeding stops) (Table 1). In these cases, sigmoid curves are fitted to the results by animal experiments. Using the inverse function of these curves, a computer simulation can be performed (Figure 1D). In the experiments that measure a change of body size, such as that caused by antiinflammatory drugs, the appropriate curve is fitted to the results by animal experiments.

Several important details to create a simulator are summarized in Appendix B. In this review, we do not deal with replicating animal behavior in simulators such as BMP-VR [4].

### 3.1. Statistical Model for Bioassay

In bioassay, the reaction rates at several doses are investigated. In our university, the presence or absence of convulsions was assessed within a specified time when lidocaine (Lid) was intraperitoneally injected into mice. The strategy to simulate probit analysis is shown in Figure 1A,B. In probit regression analysis, the cumulative distribution function (CDF) of normal distribution is fitted to these results, and the parameters (intercept [ $\alpha$ ] and slope [ $\beta$ ]) are estimated (Figure 1A) [13].

In the computer simulation, using these parameters, the distribution of minimal effective/toxic/lethal dose is determined (Figure 1B). The mean ( $\mu$ ) and standard deviation ( $\sigma$ ) of this distribution are calculated as  $-\alpha/\beta$  and  $1/\beta$ , respectively. Minimal effective/toxic/lethal dose (threshold) is set using a random number that follows this normal distribution [14]. Next, the presence or absence of response is determined. If the administered dose is greater than this threshold, it is determined that there is a response. If not, it is determined that there is no reaction (Figure 1B). Using this strategy, it is possible to create a simulator for the probit method.

In pharmacology,  $ED_{50}$ ,  $TD_{50}$ , and  $LD_{50}$  of drugs are calculated by probit method or logistic method. These values are important values in drug development [15–17]. For example, these values are used to calculate the therapeutic index. The therapeutic index is calculated as  $LD_{50}/ED_{50}$  [15] or  $TD_{50}/ED_{50}$  [16,17] and is used as an indicators of drug safety.

### 3.2. Statistical Model for Reaction Time

In this section, we introduce a statistical model for previously reported experiments measuring reaction time following drug administration. This modeling method is adapted from a previous paper [18]. These experiments include individuals who do not respond within the observation period (censored data) (Figure 1C). Survival analysis is useful for handling such censored data. The relative cumulative event is calculated using survival analysis (black line). When censored data are present, the final relative cumulative event will be less than 1. A sigmoid curve is then fitted to the results of the survival analysis (blue line in Figure 1D). Various types of curves are typically fitted to Kaplan-Meier curves; however, using relative cumulative events instead of survival rates allows for the fitting of additional sigmoid curves. Selecting the appropriate sigmoid curve to fit the obtained data is essential, and curve fitting often involves a process of trial and error.

In the computer simulation, a probability is first generated using a random number that follows a uniform distribution between 0 and 1. This probability is then used to determine the reaction time through the inverse function of the sigmoid curve (green line in Figure 1D). If the probability is equal to or greater than the asymptote ( $k$  in the Gompertz curve or  $L_{\infty}$  in the von Bertalanffy curve), the reaction time is considered infinite. Using this strategy, a simulator can be created to obtain reaction time based on these principles.

### 3.3. Limitations of These Statistical Models

The most important and common issue is that the accuracy of the statistical model depends on the quality of the results of the animal experiments. When the measurement error in animal experiments is large, the parameter values estimated in the statistical model will deviate from the actual values. As a result, the results obtained by the simulator become less reliable. It is necessary to improve the accuracy of the experiments.

In the probit method for bioassay, the log dose (minimal effective/toxic/lethal dose) is assumed to follow a normal distribution. However, although distribution of values may be skewed, the shape of the distribution is hard to determine. In statistical model for reaction time, there is a lack of theoretical background to determine what kind of curve to fit in many cases. In such cases, the curve that best fits among the multiple curves, as shown in next section, can be selected.

When creating statistical modeling, it is necessary to consider the extent to which deviation between the data and the curve is acceptable. It may be useful to compare the results of animal experiments with those of computer simulations.

## 4. Sigmoid Curves Used in Statistical Models

In this section, we describe several sigmoid curves used in statistical models and examples of their application. It is necessary to select an appropriate sigmoid curve to fit the shape of the obtained data. As described in the previous section, the necessary requirements for the fitted curve used in the statistical model are that an inverse function exists. Using this inverse function, reaction time can be calculated from randomly generated probability (Figure 1D). Herein, we describe five sigmoid curves: logistic curve, CDF of normal distribution, Gompertz curve, von Bertalanffy curve, and CDF of Weibull distribution (Tables 4 and 5). Moreover, the formulas for the inverse functions of these curves are provided, enabling the creation of simulators.

**Table 4.** Example of statistical model and proposed fitting curve.

Analysis Method	Fitting Curve	Formula
Logistic regression analysis	logistic curve	$f(x) = \frac{1}{1 + e^{-x}}$
Probit regression analysis	CDF of normal distribution	$f(x) = \Phi(x)$
	Gompertz curve	$f(x) = kg^{e^x}$
Nonlinear regression analysis	von Bertalanffy curve	$L(a) = L_{\infty} \left( 1 - e^{-k(a-t_0)} \right)$
	CDF of Weibull distribution	$F(x) = 1 - e^{-(x/\lambda)^k} \quad (x \geq 0)$ $F(x) = 0 \quad (x < 0)$
Bayesian Hierarchical model	any function	any formula

$\Phi$ : Cumulative distribution function (CDF) of the normal distribution;  $k$  in Gompertz curve: asymptote;  $L_{\infty}$  in von Bertalanffy curve: asymptote size.

**Table 5.** Examples of fitting a curve to data (not limited to pharmacology).

Fitting Curve	Contents	References
logistic curve (logistic method)	LD <sub>50</sub> : exposure time where rats die at given temperatures	[19]
	LD <sub>50</sub> : concentration of olefin at which rats die	[20]
	LD <sub>50</sub> : Monte Carlo study based on cardiac disorder data	[21]
	modeling of animal growth curve	[22]

Table 5. Cont.

Fitting Curve	Contents	References
probit curve (probit method)	radiation resistance values of microorganisms	[23]
	period of rabbit bilateral hind-limb ischemia	[24]
	effect of vasoconstrictors on local anesthetic toxicity	[25]
Gompertz curve	modeling of animal growth curve	[22]
	skin temperature after removing hand from cold water	[26]
	population modeling of tumor growth curves	[27]
	modeling of bacterial growth rate with antibiotics	[28]
von Bertalanffy curve	modeling of whelk <i>Dicathais</i> growth curve	[29]
	modeling of animal growth curve	[22,30]
	modeling of tumor growth curve	[31]
	modeling of aquatic invertebrates growth curve	[32]
	modeling of EEG phase in bipolar disorder with $\text{Li}_3\text{CO}_3$	[33]
CDF of Weibull distribution	modeling of incidence, risk factors, and heritability	[34]
	modeling of in-hospital cardiac arrest risk prediction	[35]
	modeling of failure of chicken embryo	[36]
	modeling of mechanical properties of dental materials	[37]
	modeling of drug release profiles from liposome	[38]
	modeling of drug release profiles in drug delivery system	[39]

#### 4.1. Logistic Curve

The logistic method (logistic regression analysis) is a regression analysis that uses the inverse function of logistic function (logit function). Examples of the use of the logistic method are shown in Table 5. Using the logistic method,  $\text{ED}_{50}$ ,  $\text{TD}_{50}$ , and  $\text{LD}_{50}$  are calculated from the presence or absence of a reaction to drugs. In previous studies,  $\text{LD}_{50}$  was calculated based on various factors, including the time of exposure at a given temperature that resulted in death in 50% of the animals within 24 h after heating [19], the concentration of olefin (metabolites of sevoflurane) at which 50% of Wistar rats died [20], and a Monte Carlo study using data from cardiac disorder patients [21]. Moreover, logistic curve fitting can be performed on the data. In a previous study, a logistic curve was fitted to the body weight and chest circumference of sheep [22]. The logistic function finds applications in a range of fields, including biology, biomathematics, chemistry, demography, economics, geoscience, mathematical psychology, probability, sociology, political science, linguistics, statistics, and artificial neural networks.

The logistic function was introduced by Pierre-François Verhulst [40]. It is a function that converts any real number (ranging from  $-\infty$  to  $+\infty$ ) to a probability value (ranging from 0 to 1). Logistic function is the inverse function of logit (logistic unit). The standard logistic function is expressed by the following formula:

$$f(x) = \frac{1}{1 + e^{-x}} \quad (1)$$

The graph of the standard logistic function is shown in Figure 2 (red line).

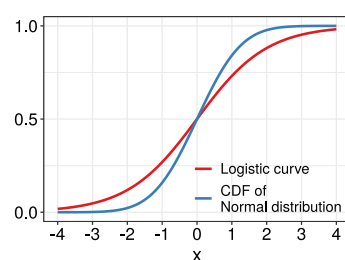


Figure 2. Standard logistic curve and cumulative distribution function (CDF) of normal distribution.



The logit function is expressed by the following formula:

$$\text{logit}(p) = \begin{cases} -\infty & (p = 0) \\ \log\left(\frac{p}{1-p}\right) & (0 < p < 1) \\ \infty & (p = 1) \end{cases} \quad (2)$$

#### 4.2. CDF of Normal Distribution

The probit method (probit regression analysis) is a regression analysis that uses the inverse function of CDF of normal distribution (probit function). Examples of the use of the probit method are shown in Table 5. The probit method is used to analyze the relationship between pesticide concentration and insect mortality in biology [41]. The probit method is also used to analyze metal fatigue in the field of materials science [42], radiation resistance values of microorganisms [23], the period of rabbit bilateral hind-limb ischemia [24], and the effect of vasoconstrictors on local anesthetic toxicity [25].

CDF of normal distribution is a function that converts any real number (ranging from  $-\infty$  to  $+\infty$ ) to a probability value (ranging from 0 to 1). CDF of the standard normal distribution ( $\Phi$ ) is expressed by the following formula:

$$\Phi(x) = \frac{1}{\sqrt{2\pi}} \int_{-\infty}^x e^{-\frac{y^2}{2}} dy = \frac{1}{2} \left[ 1 + \text{erf}\left(\frac{x}{\sqrt{2}}\right) \right] \quad (3)$$

where erf is the error function (Equations (A1) and (A2)). In practice, when performing calculations using a computer, several approximate formulas are used (for example, Equation (A3)). The graph of the CDF of the normal distribution is shown in Figure 2 (blue line). The graph has a narrower base than that of the standard logistic curve.

The inverse function of the CDF of the standard normal distribution is called the probability unit (probit) function. Probit converts a probability value (ranging from 0 to 1) to any real number (ranging from  $-\infty$  to  $+\infty$ ). The probit function is expressed by the following formula:

$$\Phi^{-1}(p) = \begin{cases} -\infty & (p = 0) \\ \sqrt{2} \text{erf}^{-1}(2p - 1) & (0 < p < 1) \\ \infty & (p = 1) \end{cases} \quad (4)$$

where  $\text{erf}^{-1}$  is the inverse error function (Equation (A4)). In practice, several approximate formulas are used (for example, Equation (A5)).

#### 4.3. Gompertz Curve

The Gompertz curve is a sigmoid function that describes growth as being slowest at the start and end of a given time period. The right-side or future value asymptote of the function is approached much more gradually by the curve than the left-side or lower-valued asymptote. The Gompertz curve was originally designed to describe human mortality as  $L_x = kg^{c^x}$  by Benjamin Gompertz [43]. Winsor demonstrated the mathematical properties of the Gompertz curve and summarized examples of applying this curve to organism growth, psychological growth, population growth, and economic growth [44]. Moreover, the Gompertz curve has been modified for use in biology, with regard to detailing populations. The Gompertz curve is widely used in physiology, particularly in modeling growth curves. It is commonly applied to describe the growth patterns of animals. Examples of the use of the Gompertz curve are shown in Table 5. The Gompertz curve has been fitted to recovery palm skin temperature data of human subjects, which was collected after removing the hand

from cold water [26], as well as several growth curves such as those for sheep growth [22] and tumor growth [27]. In pharmacology, the Gompertz curve has been fitted to bacterial growth rate in the presence of antibiotics [28].

In R software (version  $\geq 1.2.3$ ), the Gompertz curve is defined using the following formula:

$$f(x) = \text{Asym} \cdot e^{-b_2 \cdot b_3^x} \tag{5}$$

where Asym is asymptote,  $b_2$  is the displacement along the x-axis, and  $b_3$  is the growth rate. A graph of the Gompertz curve is shown in Figure 3.

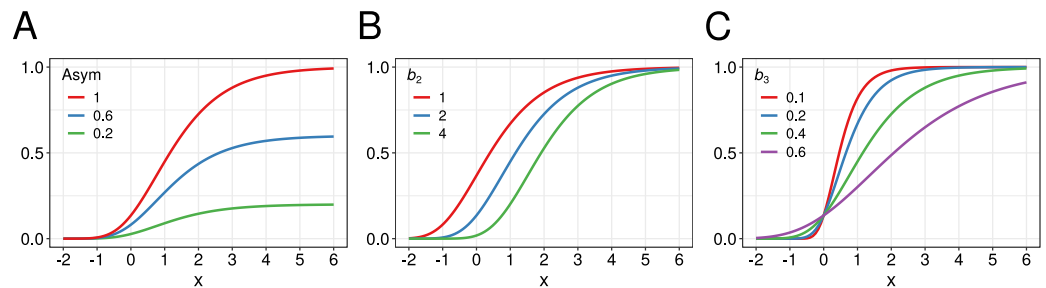


**Figure 3.** Gompertz curve:  $f(x) = \text{Asym} \cdot e^{-b_2 \cdot b_3^x}$  (Equation (5)). (A) Graph when  $b_2 = 2$  and  $b_3 = 0.2$  and Asym is changed, (B) Graph when Asym = 1 and  $b_3 = 0.4$  and  $b_2$  is changed, (C) Graph when Asym = 1 and  $b_2 = 2$  and  $b_3$  is changed.

The inverse function of the Gompertz curve is expressed by the following formula:

$$f^{-1}(x) = \begin{cases} \frac{\log\left(\log \frac{\text{Asym}}{x} / b_2\right)}{\log b_3} & (0 < x < \text{Asym}) \\ \infty & (x \geq \text{Asym}) \end{cases} \tag{6}$$

#### 4.4. Von Bertalanffy Curve

The von Bertalanffy curve (or von Bertalanffy growth function) is a type of growth curve for a time series. It is named after Ludwig von Bertalanffy [45]. Examples of the use of the von Bertalanffy curve are shown in Table 5. The von Bertalanffy curve has been fitted to the data of whelk Dicathais growth [29], sheep growth [22], the growth of chickens used for meat [30], tumor growth [31], and aquatic invertebrates [32]. In pharmacology, the von Bertalanffy curve has been fitted to the data of ElectroEncephaloGraphy (EEG) phase growth in bipolar disorder with lithium carbonate [33].

The von Bertalanffy curve is expressed by the following formula:

$$L(a) = L_\infty \left(1 - e^{-k(a-t_0)}\right) \tag{7}$$

where  $a$  is age,  $k$  is the growth coefficient,  $t_0$  is the theoretical age when size is zero, and  $L_\infty$  is asymptotic size. A graph of the von Bertalanffy curve is shown in Figure 4.

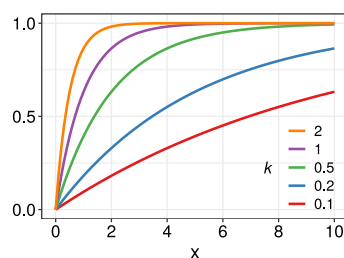


**Figure 4.** von Bertalanffy curve:  $L(x) = L_\infty \left(1 - e^{-k(x-t_0)}\right)$  (Equation (7)). Graph when  $L_\infty = 1$  and  $t_0 = 0$  and  $k$  is changed.

The inverse function of the von Bertalanffy curve is expressed by the following formula:

$$f^{-1}(x) = \begin{cases} t_0 - \frac{\log\left(1 - \frac{x}{L_\infty}\right)}{k} & (0 \leq x < L_\infty) \\ \infty & (x \geq L_\infty) \end{cases} \quad (8)$$

#### 4.5. CDF of the Weibull Distribution

The Weibull distribution is named after Waloddi Weibull [46]. It was first applied to describe a particle size distribution by Rosin and Rammler [47]. A Weibull curve describes a broad range of random variables, especially those related to the time to failure or the time between events. Examples of its use are shown in Table 5. The CDF of the Weibull distribution has been applied to investigate various subjects including the failure of chicken embryos to survive incubation [36]; incidence, risk factors, and heritability estimates of hind limb lameness caused by hip dysplasia [34]; in-hospital cardiac arrest [35]; and the mechanical properties of dental materials affected by gastric acid [37]. In pharmacology, the CDF of the Weibull distribution has been fitted to the data of drug release profiles from liposome [38] and drug release profiles in drug delivery system [39].

The CDF of the Weibull distribution is expressed by the following formula:

$$F(x) = \begin{cases} 1 - e^{-(x/\lambda)^k} & (x \geq 0) \\ 0 & (x < 0) \end{cases} \quad (9)$$

where  $k > 0$  is the shape parameter and  $\lambda > 0$  is the scale parameter of the distribution. The graph of the CDF of the Weibull distribution is shown in Figure 5.

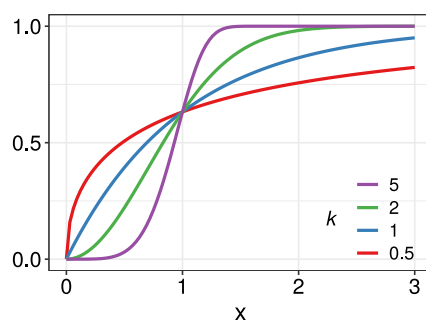


**Figure 5.** CDF of Weibull distribution:  $F(x) = 1 - e^{-(x/\lambda)^k}$  ( $x \geq 0$ ) (Equation (9)). Graph when  $\lambda = 1$  and  $k$  is changed.

The inverse function of the CDF of the Weibull distribution is expressed by the following formula:

$$F^{-1}(p) = \begin{cases} \lambda(-\log(1 - p))^{\frac{1}{k}} & (0 \leq p < 1) \\ \infty & (p = 1) \end{cases} \quad (10)$$

#### 4.6. Comparison of Sigmoid Curves

Both the logistic curve and the CDF of the normal distribution are point-symmetry centered at  $y = 0.5$  (Figure 2). In contrast, because the Gompertz curve and CDF of the Weibull curve are asymmetric sigmoid curves (Figures 3 and 5); these curves are considered to be widely applicable compared to logistic curves and CDFs of normal distribution. Moreover, because the von Bertalanffy curve is not a sigmoid curve, its application is thought to be limited.

When there is no theoretical background for the distribution of data, it is recommended to perform NLS on the experimental data to fit multiple curves and then adopt the curve that best fits using the values such as the coefficient of determination ( $R^2$ ) [22,36,38,39] and Akaike Information Criterion (AIC) [27].

## 5. Hierarchical Bayesian Model

If the statistical model is too complex to perform a regression analysis, hierarchical Bayesian model is available. The hierarchical Bayesian model can be used instead of generalized linear model (GLM) or generalized linear mixed model (GLMM), and nonlinear regression analysis. Moreover, more flexible modeling is possible in a hierarchical Bayesian model. Then, the posterior distributions of parameters are estimated by Hamiltonian Monte Carlo (HMC) simulation.

Hierarchical Bayesian models are used in many areas such as clinical trials [48–51], animal experiments [52–54], and genetics [55,56]. Regarding the creation of statistical models for simulators, there are models for reproducing the movement of the myocardium [54,57]. In this section, we will introduce the statistical models of our recent studies [7,8], and the simulator [12].

### 5.1. Advantages of Using the Hierarchical Bayesian Model in a Computer Simulation

In a computer simulation (including the simulator for pharmacological education), the parameters for each individual are generated by random number generators. Therefore, the distribution of the parameters must be specified. In GLM, GLMM, and nonlinear regression analysis, the mean and standard error of these parameters can be estimated. However, the distribution of these estimated parameters is unknown, although a normal distribution is assumed.

The distribution of parameters can be assumed by the researchers and the hyperparameters that determine the shape of this distribution can be estimated in a hierarchical Bayesian model. The parameters can be generated using the appropriate random number generator that follows this distribution and hyperparameters in the computer simulation. This is one of the advantages of the hierarchical Bayesian model.

### 5.2. Example of a Statistical Model Using Hierarchical Bayesian Model

Recently, we reported the statistical models and the results of computer simulation for local anesthetic agents [7,8]. Here, we explain their theoretical background and assumed model (Figure 6).

#### 5.2.1. Statistical Model for Local Anesthetic Agents and Parameter Estimation

The methods of animal experiments for local anesthetic agents are described below. This is a modified description based on a previous study [7].

- (1) Shave the hair on the back of the guinea pig
- (2) Inject 0.1 mL of saline and 5 drugs intradermally: procaine (Pro), lidocaine (Lid), mepivacaine (Mep), bupivacaine (Bup), and Lid + adrenaline
- (3) Mark each injection site papule enclosed in a circle using a magic marker
- (4) Stimulate six times at each papule with a needle. Count the number of skin contractions. This number is defined as the score. The score value is 0 to 6.
- (5) Stimulate at 5 min intervals up to 120 min. When a score of 6 is obtained three times in a row, the stimulation is finished, and that time is defined as the duration

From this animal experiment, the score values are obtained. The CDF of the normal distribution is fitted to these results for each drug and individual (Figure 6A). Thereafter, the parameter values ( $\mu$  and  $\sigma$ ) are estimated for each drug and individual. To estimate

these parameters, the statistical model is assumed, and the hyperparameters that determine the distribution of  $\mu$  and  $\log \sigma$  ( $\mu_0$  and  $s_\mu$  for  $\mu$ ;  $\log \sigma_0$  and  $s_{\log \sigma}$  for  $\log \sigma$ ) are estimated by the Hamiltonian Monte Carlo simulation (Figure 6B).

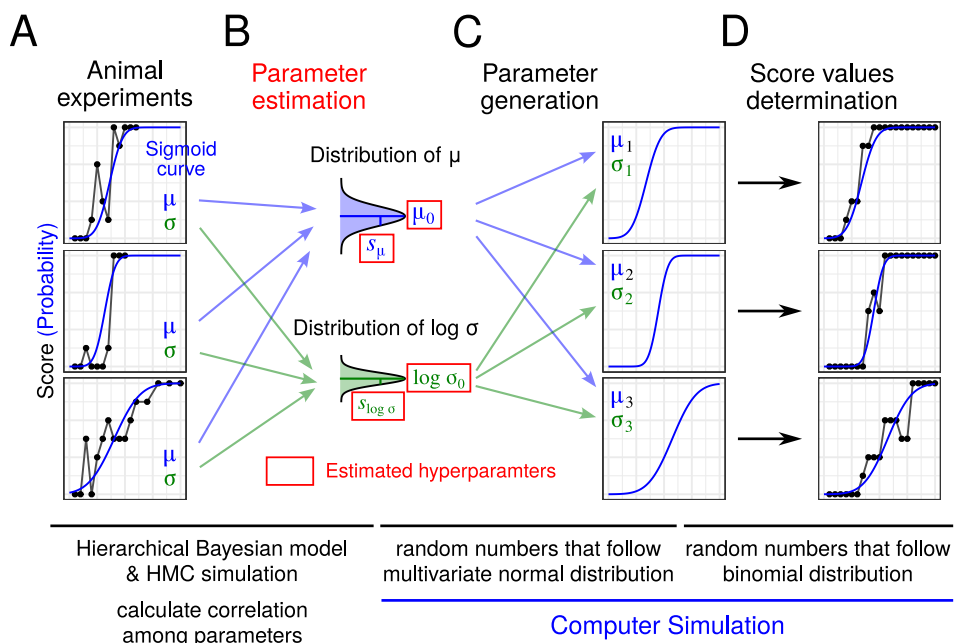


**Figure 6.** Strategy used in the simulation for local anesthetic agents using a hierarchical Bayesian model. (A) Fitting the sigmoid curve (CDF of normal distribution) to each result of animal experiments. The curve shows the probability of responding to a stimulus at any time. The parameters that determine the shape of the curve are the mean ( $\mu$ ) and standard deviation ( $\sigma$ ). (B) Estimation of parameters: The distributions of these parameters ( $\mu$  and  $\sigma$ ) are estimated by hierarchical Bayesian model and Hamiltonian Monte Carlo (HMC) simulation. Estimated hyperparameters are  $\mu_0$  and  $s_\mu$  for the distribution of  $\mu$ , and  $\log \sigma_0$  and  $s_{\log \sigma}$  for the distribution of  $\sigma$ . In addition, correlation coefficients among these parameters are calculated. (C,D) Computer simulation procedure: The parameters for simulation ( $\mu_i$  and  $\sigma_i$ ) are set using the random number generator that follows to multivariate normal distribution. The shape of cumulative normal distribution curve for each individual is determined by the values of generated  $\mu$  and  $\sigma$  (C). The number of reactions to a stimulus (score value) are determined by the random number generator that follows to binomial distribution (D). This strategy is modification of previous studies [7,8].

These hyperparameters are required to generate parameters of each drug and individual in the computer simulation. Therefore, it is desirable to assume simple distributions for  $\mu$  and  $\sigma$ . In our previous study, we assumed that  $\mu$  follows a normal distribution and  $\sigma$  follows a lognormal distribution (i.e.,  $\log \sigma$  follows a normal distribution) [7].

The statistical model for this experiment is assumed as follows (modified and corrected the description in reference [7]):

- (1) Drug concentration in local tissue decreases exponentially. This concentration is determined by elapsed time ( $t$ ) and the presence or absence of adrenaline ( $\text{adr} \times V_{\text{adr}}$ ) (Equation (11)). When adrenaline is present, the rate of decrease in local concentration becomes smaller (the slope is decreased). Initial log concentration and slope were set to 100 and  $-1$ , respectively.

$$\text{Concentration} = 100 - (1 - \text{adr} \times V_{\text{adr}})t \tag{11}$$

where

$t$  is time (minute)

$V_{\text{adr}}$  is the dummy variable for adrenaline  
(0 when adrenaline is absent, 1 when adrenaline is present).

- (2) The probability of reacting to needle stimulation ( $p$ ) is determined as the upper probability of normal distribution (mean is  $\mu[i, j]$  and SD is  $\sigma[i, j]$ ) based on drug concentration at stimulation time (Equation (12)). The number of reactions to stimulation (score value,  $\text{Score}[i, j]$ ) follows a binomial distribution at this probability (Equation (13)).

$$p = 1 - \Phi\left(\frac{\text{Concentration} - \mu[i, j]}{\sigma[i, j]}\right) \quad (12)$$

$$\text{Score}[i, j] \sim \text{Bi}(p, 6) \quad (13)$$

where

$i = 1, 2, 3, 4$  (drug number; 1: Pro; 2, Lid; 3, Mep, 4: Bup)

$j = 1, 2, \dots, 51$  (individual number)

Bi is the probability mass function for the binomial distribution.

- (3) The parameters ( $\mu[i, j]$  and  $\sigma[i, j]$ ) for distribution of each drug and individual follow normal and lognormal distributions, respectively (Figure 6B).  $\mu[i, j]$  follows a normal distribution (mean is  $\mu_0$  and SD is  $s_\mu$ ) (Equation (14)). As  $\sigma[i, j]$  must be positive,  $\sigma[i, j]$  was assumed to follow a lognormal distribution (mean is  $\log \sigma_0[i]$  and SD is  $s_{\log \sigma}[i]$ ) (Equation (15)).

$$\mu[i, j] \sim \text{Normal}(\mu_0[i], s_\mu[i]) \quad (14)$$

$$\sigma[i, j] \sim \text{LogNormal}(\log \sigma_0[i], s_{\log \sigma}[i]) \quad (15)$$

- (4) The following distributions are assumed for the prior distribution of parameters.  $\mu_0[i]$  follows a Cauchy distribution (Equation (16)).  $s_\mu[i]$  follows a half Cauchy distribution (Equation (17)).  $\log \sigma_0[i]$  follows a normal distribution (Equation (18)).  $s_{\log \sigma}[i]$  and  $\text{adr}$  follow uniform distributions (Equations (19) and (20)).

$$\mu_0[i] \sim \text{Cauchy}(50, 20) \quad (16)$$

$$s_\mu[i] \sim \text{HalfCauchy}(0, 1) \quad (17)$$

$$\log \sigma_0[i] \sim \text{Normal}(2.5, 1) \quad (18)$$

$$s_{\log \sigma}[i] \sim \text{Uniform}(> 0) \quad (19)$$

$$\text{adr} \sim \text{Uniform}(0, 1) \quad (20)$$

### 5.2.2. Computer Simulation for Local Anesthetic Agents

Using the hyperparameters estimated by HMC simulation, the parameters ( $\mu$  and  $\sigma$ ) in each drug and individual were generated by a random number generator (Figure 6C). Since the shape of the CDF of the normal distribution is determined by these generator parameters, the probability can be calculated at any time. Then, the number of reactions to a stimulus (score values) is determined by a random number generator that follows a binomial distribution at specified time intervals (Figure 6C). From the obtained score values, the duration of the drug is determined.

In the simulator, the reaction is determined by accounting to a random number that follows a Bernoulli distribution based on the calculated probability:

The computer simulation is performed as follows (modified from the description in a previous study [7]):

- (1) the parameters ( $\mu[i, j]$  and  $\sigma[i, j]$ ) are generated by a random number generator following a normal or lognormal distribution, respectively.
  - $i = 1, 2, 3, 4$  (drug number; 1: Pro; 2, Lid; 3, Mep, 4: Bup)
  - $j = 1, 2, \dots, 100$  (individual number)
- (2) score values are determined by a random number generator following a binomial distribution for this probability
  - determine how many responses occur when stimulated six times
- (3) repeat this operation 100 times (for 100 individuals)
- (4) determine the duration of each drug and individual
  - compare the median of duration among drugs by survival analysis
  - evaluate the differences in duration among drugs and the effect of a vasoconstrictor (adrenaline) on duration

In the survival analysis, the results obtained from the computer simulation were similar to those from the animal experiments (Figure 7) since the parameter values were properly adjusted [7]. These findings suggest that the simulator, utilizing this statistical model, can serve as a viable alternative to animal experiments in pharmacological education.

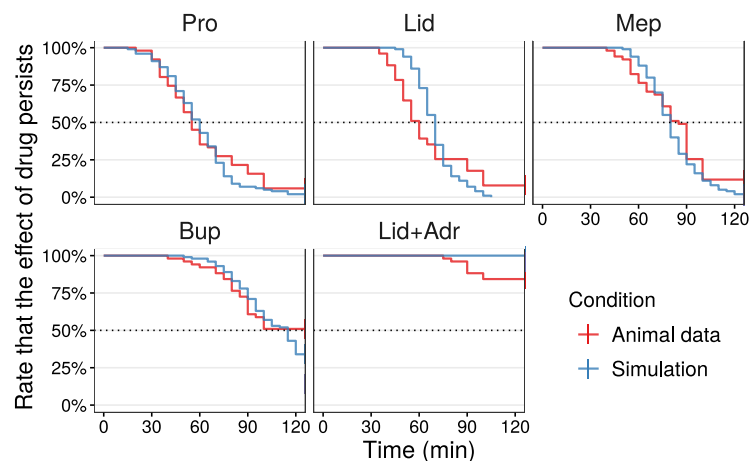


**Figure 7.** A comparison of the results by survival analysis between animal experiments and computer simulation. These results are modifications of previous study [7].

### 5.2.3. Improved Statistical Model Considering the Correlation Among Parameters

The simulation described in the previous section does not consider the correlation among parameters—the parameter values were generated by random numbers with the correlation coefficients between drugs set to zero (Figure 8: upper panel). However, individuals who tend to respond to one local anesthetic agent are likely to respond to other drugs, and the duration of drugs is also correlated. Therefore, it is desirable to consider this correlation when creating a simulator.

In our recent study [8], the correlations among estimated parameters were investigated: (1) correlation among  $\mu$  in all drugs ( $r_{ij}$ ), (2) correlation among  $\log \sigma$  in all drugs ( $s_{ij}$ ), and (3) correlation between  $\mu$  and  $\log \sigma$  in each drug ( $u_i$ ). In the computer simulation, the parameters in each individual were generated using a random number generator that follows the multivariate normal distribution. For generating parameters, the correlation matrix is set using these correlation coefficients (Figure 8: lower left). Next, the score values and duration were determined. By accounting for the correlation among drugs, the correlation in duration among drugs was enhanced (Figure 8: lower right). These results suggest that parameter generation considering the correlation among parameters is

important to reproduce the results of animal experiments in the computer simulation and the simulator.

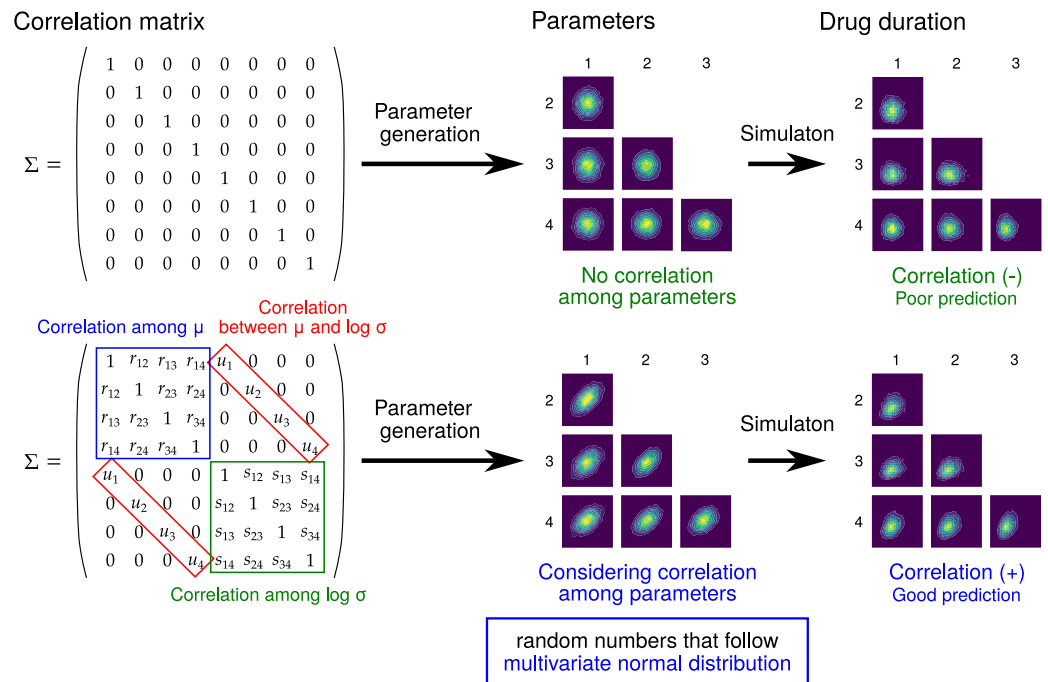


**Figure 8.** The strategy used in the simulation for local anesthetic agents. (Left) Correlation matrix among parameters estimated by animal experiments is shown. In this case, the correlations (1) among  $\mu$  of drugs ( $r_{ij}$  in blue box), (2) among  $\log \sigma$  of drugs ( $s_{ij}$  in green box), and (3) between  $\mu$  and  $\log \sigma$  ( $u_i$  in red box) are set. Using this correlation matrix, the parameters are set by generating random numbers that follow the multivariate normal distribution. (Middle) The distributions of generated parameters are shown. A case without considering these correlations is shown in the upper panel, and a case considering these correlations is shown in the lower panel. (Right) Correlations of drug duration obtained by the computer simulation are shown for the case without considering the correlations (Upper panel) and for the case considering the correlations (Lower panel).

Recently, we created a simulator for local anesthetic agents based on this improved statistical model as a web-based simulator [12]. We hope that this simulator is an effective alternative to animal experiments in pharmacological education.

### 6. Conclusions

In this review, we introduced the simulators used in pharmacological education, as well as two types of strategies (bioassay and experiments that measure reaction time) for creating simulators of animal experiments. We also described five sigmoid curves (for fitting the relative cumulative event by survival analysis) and their inverse functions. Using this strategy, it is possible to develop a simulator that predicts reaction times following drug administration. Additionally, a statistical model for local anesthetic agents, utilizing a hierarchical Bayesian approach, was demonstrated. Considering the correlation among estimated parameters, it is possible to create simulators that give results more similar to those of animal experiments. We hope this review will be useful when creating a simulator in pharmacological education. The pharmacological education will be possible by these simulators at educational institutions where animal experiments are difficult due to various restrictions. If these simulators are used in a variety of educational institutions, it is expected that the number of simulator-based education programs will increase in the future.

**Author Contributions:** Conceptualization, T.A.; methodology, T.A.; writing—original draft preparation, T.A.; writing—review and editing, T.A. and H.K.; visualization, T.A. and H.K.; supervision,



T.A.; project administration, T.A.; funding acquisition, T.A. All authors have read and agreed to the published version of the manuscript.

**Funding:** This research was funded by a Scientific Research Special Grant from Matsumoto Dental University.

**Institutional Review Board Statement:** Not applicable.

**Informed Consent Statement:** Not applicable.

**Data Availability Statement:** Not applicable.

**Acknowledgments:** We thank Norio Sogawa (Institution of Oral Science, Matsumoto Dental University) and all students for obtaining the animal data in practice of pharmacology.

**Conflicts of Interest:** The authors declare no conflict of interest.

## Abbreviations

The following abbreviations are used in this manuscript:

ED <sub>50</sub>	effective dose 50%
TD <sub>50</sub>	toxic dose 50%
LD <sub>50</sub>	lethal dose 50%
CDF	cumulative distribution function
SD	standard deviation

## Appendix A. Approximate Formulas

### Appendix A.1. CDF of the Standard Normal Distribution

- Error function [58]

$$\operatorname{erf}(x) = \frac{2}{\sqrt{\pi}} \int_0^x e^{-t^2} dt \quad (\text{A1})$$

- Error function (Taylor series) [58,59]

$$\operatorname{erf}(x) = \frac{2}{\sqrt{\pi}} \sum_{n=0}^{\infty} \frac{(-1)^n x^{2n+1}}{n!(2n+1)} = \frac{2}{\sqrt{\pi}} \left( z - \frac{z^3}{3} + \frac{z^5}{10} - \frac{z^7}{42} + \frac{z^9}{216} - \dots \right) \quad (\text{A2})$$

- Approximation formula of normal probability function in Abramowitz and Stegun 26.2.17 [60]

$$P(x) = 1 - Z(x)(b_1 t_1 + b_2 t_2 + b_3 t_3 + b_4 t_4 + b_5 t_5) + \epsilon(x) \quad (\text{A3})$$

$$Z(x) = \frac{1}{\sqrt{2\pi}} e^{-\frac{x^2}{2}}, \quad t = \frac{1}{1 + px}$$

$$|\epsilon(x)| < 7.5 \times 10^{-8}$$

$$p = 0.2316419$$

$$b_1 = 0.319381530, \quad b_2 = -0.356563782, \quad b_3 = 1.781477937$$

$$b_4 = -1.821255978 \quad b_5 = 1.330274429$$

### Appendix A.2. Probit Function

- Inversed Error function (Taylor series) [61]

$$\operatorname{erf}^{-1}(x) = \frac{\sqrt{\pi}}{2} \left( z + \frac{\pi}{12} z^3 + \frac{7\pi^2}{480} z^5 + \frac{127z^7}{42} + \frac{4369\pi^4}{5806080} z^9 + \frac{34807\pi^5}{182476800} z^{11} + \dots \right) \quad (\text{A4})$$

- Approximation formula of probit function by Toda [62]

$$u(p) \cong \left[ y(b_0 + b_1y + b_2y^2 + \dots + b_{10}y^{10}) \right]^{\frac{1}{2}} \quad (\text{A5})$$

$$y = -\log 4p(1-p)$$

$$\begin{aligned} b_0 &= 0.1570796288, & b_1 &= 0.3706987906 \times 10^{-1} \\ b_2 &= -0.8364353589 \times 10^{-3}, & b_3 &= -0.2250947176 \times 10^{-3} \\ b_4 &= 0.6841218299 \times 10^{-5}, & b_5 &= 0.5824238515 \times 10^{-5} \\ b_6 &= -0.1045274970 \times 10^{-5}, & b_7 &= 0.8360937017 \times 10^{-7} \\ b_8 &= -0.3231081277 \times 10^{-8}, & b_9 &= 0.3657763036 \times 10^{-10} \\ b_{10} &= 0.69362339826 \times 10^{-12} \end{aligned}$$

## Appendix B. Things to Consider When Creating a Simulator

There are several things to consider when creating a simulator for pharmacological education:

- (1) Distribution of parameters—Which distribution do parameters follow?
- (2) Selection of program language including execution environment
- (3) Function to generate random numbers including the usage of extra packages

(1) As previously described, the distribution of parameters is the most important factor. Since the parameters are generated using this distribution, the distribution must be simple enough to be generated by a computer program. In many cases, the parameters are assumed to follow a normal distribution or lognormal distribution.

(2) The selection of program language should be considered. If the simulator is written using R or Python programming languages, these languages must be installed in the computer or bundled with the simulator. If the simulator is written using C/C++ languages, this simulator must be compiled in each operating system including Windows, Mac, and Linux. Therefore, these simulators are environment dependent. If the simulator is written by JavaScript/TypeScript languages, the simulator is environment-independent since it runs on a web browser.

(3) It is important to confirm whether the functions to generate random numbers—including the usage of extra packages—exist or not. In many cases, it is sufficient to have functions for a random numbers that follow uniform distribution for the probability and normal distribution and lognormal distribution for the parameters. However, the function for a random number generator that follows a multivariate normal distribution may be required [8]. For reference, the packages/library for generating random numbers that follow the multivariate normal distribution are detailed in the following section.

### *External Packages for Multivariate Normal Distribution*

The following list is some representative packages/libraries for generating random numbers that follow multivariate normal distribution in various languages:

- C++: EigenMultivariateNormal function in Eigen library [63]
- R: rmvnorm function in mvtnorm package [64]
- Python: random.multivariate\_normal function in numpy package [65]
- JavaScript/TypeScript: MultivariateNormal function in multivariate-normal package [66]

## References

1. Council, N.R. *Guide for the Care and Use of Laboratory Animals: Eighth Edition*; The National Academies Press: Washington, DC, USA, 2011. [CrossRef]
2. University of Strathclyde. Strathclyde Pharmacology Simulations. Available online: [http://spider.science.strath.ac.uk/sipbs/page.php?page=software\\_sims](http://spider.science.strath.ac.uk/sipbs/page.php?page=software_sims) (accessed on 28 October 2024).
3. eGrid Corporation. Pharmaco-PICOS: Pharmacological Practice of Intestine and Cardiovascular Organ Simulator. Available online: <https://pharmaco-picos.education> (accessed on 28 October 2024).
4. ERISA. BMP-VR: Basic Medicine Practice-Virtual Reality. Available online: <https://jstories.media/article/animal-experiments> (accessed on 28 October 2024).
5. Certara. Simcyp™: PBPK Tech-Driven Services Predict Clinical Outcomes from Virtual Populations. Available online: <https://www.certara.com/services/simcyp-pbpbk> (accessed on 28 October 2024).
6. Plus, S. PKPlus™ Module Extends GastroPlus®: PBPK & PBBM Modeling Software. Available online: <https://www.simulations-plus.com/software/gastroplus/pk-models> (accessed on 28 October 2024).
7. Ara, T.; Kitamura, H. Development of a Predictive Statistical Pharmacological Model for Local Anesthetic Agent Effects with Bayesian Hierarchical Model Parameter Estimation. *Medicines* **2023**, *10*, 61. [CrossRef]
8. Ara, T.; Kitamura, H. Improvement of local anesthetics agents' simulation using Monte Carlo simulation considering correlation among parameters. *Biomedinformatics* **2024**, *4*, 2133–2148. [CrossRef]
9. Ezeala, C.C. Integration of computer-simulated practical exercises into undergraduate medical pharmacology education at Mulungushi University, Zambia. *J. Educ. Eval. Health Prof.* **2020**, *17*, 1–9. [CrossRef]
10. Andrews, L.B.; Barta, L. Simulation as a Tool to Illustrate Clinical Pharmacology Concepts to Healthcare Program Learners. *Curr. Pharmacol. Rep.* **2020**, *6*, 182–191. [CrossRef]
11. Borghardt, J.M.; Weber, B.; Staab, A.; Kloft, C. Pharmacometric Models for Characterizing the Pharmacokinetics of Orally Inhaled Drugs. *AAPS J.* **2015**, *14*, 853–870. [CrossRef]
12. Ara, T. simla-ts (Ver 2.1.0). 2024. Available online: [https://toshi-ara.github.io/simla-ts/sim\\_local\\_anesthetics.html](https://toshi-ara.github.io/simla-ts/sim_local_anesthetics.html) (accessed on 23 October 2024).
13. Wooldridge, J.M. *Introductory Econometrics: A Modern Approach*, 4th ed.; South-Western Cengage Learning: Boston, MA, USA, 2009; Chapter 15.
14. Iwaya, T.; Tanaka, T. Monte Carlo Simulation and Distribution Characteristics of the Estimates by Probit and Staircase Methods [in Japanese]. *J. Soc. Mater. Sci. Jpn.* **1990**, *39*, 914–920. [CrossRef]
15. Ritteri, J.; Flower, R.; Henderson, G.; Loke, Y.K.; MacEwan, D.; Rang, H. *Rang & Dale's Pharmacology*, 9th ed.; Elsevier: Amsterdam, The Nederland, 2019.
16. Brunton, L.; Knollman, B.C. *Pharmacological Basis of Therapeutics*, 14th ed.; McGraw-Hill Education: New York City, NY, USA, 2022.
17. Golan, D.E.; Tashjian, A.H., Jr.; Armstrong, E.J.; Armstrong, A.W. *Principles of Clinical Pharmacology: The Pathophysiologic Basis of Drug Therapy*, 3rd ed.; Lippincott Williams & Wilkins: Philadelphia, PA, USA, 2011.
18. Kawanishi, D.T.; Brinker, J.A.; Reeves, R.; Kay, G.N.; Gross, J.; Pioger, G.; Petitot, J.C.; Esler, A.; Grunkemeier, G. Cumulative Hazard Analysis of J-Wire Fracture in the Accufix Series of Atrial Permanent Pacemaker Leads. *Pacing Clin. Electrophysiol.* **1998**, *21*, 2322–2326. [CrossRef]
19. Lord, P.F.; Kapp, D.S.; Hayes, T.; Weshler, Z. Production of systemic hyperthermia in the rat. *Eur. J. Cancer Clin. Oncol.* **1984**, *20*, 1079–1085. [CrossRef]
20. Gonsowski, C.T.; Laster, M.J.; Eger, E.I.; Ferrell, L.D.; Kerschmann, R.L. Toxicity of Compound A in Rats: Effect of a 3-Hour Administration. *Anesthesiology* **1994**, *80*, 556–565. [CrossRef]
21. Peduzzi, P.; Concato, J.; Kemper, E.; Holford, T.R.; Feinstein, A.R. A simulation study of the number of events per variable in logistic regression analysis. *J. Clin. Epidemiol.* **1996**, *49*, 1373–1379. [CrossRef]
22. Li, J.; Shan, X.; Chen, Y.; Xu, C.; Tang, L.; Jiang, H. Fitting of Growth Curves and Estimation of Genetic Relationship between Growth Parameters of Qianhua Mutton Merino. *Genes* **2024**, *15*, 390. [CrossRef]
23. Anellis, A.; Werkowski, S. Estimation of Radiation Resistance Values of Microorganisms in Food Products. *Appl. Microbiol.* **1968**, *16*, 1300–1308. [CrossRef]
24. Little, R.A. Resistance to post-traumatic fluid loss at different ages. *Br. J. Exp. Pathol.* **1972**, *53*, 341–346.
25. Taylor, S.E.; Dorris, R.L. Modification of local anesthetic toxicity by vasoconstrictors. *Anesth. Prog.* **1989**, *36*, 79–87.
26. Verma, S.S.; Gupta, R.K.; Nayar, H.S.; Rai, R.M. Gompertz curve in physiology: An application. *Indian J. Physiol. Pharmacol.* **1982**, *26*, 47–53.
27. Vaghi, C.; Rodallec, A.; Fanciullino, R.; Ciccolini, J.; Mochel, J.P.; Mastri, M.; Ebos, J.M.L.; Benzekry, S. Population modeling of tumor growth curves and the reduced Gompertz model improve prediction of the age of experimental tumors. *PLoS Comput. Biol.* **2020**, *16*, e1007178. [CrossRef]

28. Ogunrinu, O.J.; Norman, K.N.; Vinasco, J.; Levent, G.; Lawhon, S.D.; Fajt, V.R.; Volkova, V.V.; Gaire, T.; Poole, T.L.; Genovese, K.J.; et al. Can the use of older-generation beta-lactam antibiotics in livestock production over-select for beta-lactamases of greatest consequence for human medicine? An in vitro experimental model. *PLoS ONE* **2020**, *15*, e0242195. [[CrossRef](#)]
29. Phillips, B.F.; Campbell, N.A. A new method of fitting the von Bertalanffy growth curve using data on the whelk *Dicathais*. *Growth* **1968**, *32*, 317–329.
30. Kühleitner, M.; Brunner, N.; Nowak, W.G.; Renner-Martin, K.; Scheicher, K. Best-fitting growth curves of the von Bertalanffy-Pütter type. *Poult. Sci.* **2019**, *98*, 3587–3592. [[CrossRef](#)]
31. Kühleitner, M.; Brunner, N.; Nowak, W.G.; Renner-Martin, K.; Scheicher, K. Best fitting tumor growth models of the von Bertalanffy-Pütter Type. *BMC Cancer* **2019**, *12*, 683. [[CrossRef](#)]
32. Lee, L.; Atkinson, D.; Hirst, A.G.; Cornell, S.J. A new framework for growth curve fitting based on the von Bertalanffy Growth Function. *Sci. Rep.* **2020**, *10*, 7953. [[CrossRef](#)]
33. Demirer, R.M.; Kesebir, S. The entropy of chaotic transitions of EEG phase growth in bipolar disorder with lithium carbonate. *Sci. Rep.* **2021**, *11*, 11888. [[CrossRef](#)]
34. van Hagen, M.A.E.; Ducro, B.J.; van den Broek, J.; Knol, B.W. Incidence, risk factors, and heritability estimates of hind limb lameness caused by hip dysplasia in a birth cohort of boxers. *Am. J. Vet. Res.* **2005**, *66*, 307–312. [[CrossRef](#)]
35. Kim, J.; Park, Y.R.; Lee, J.H.; Lee, J.H.; Kim, Y.H.; Huh, J.W. Development of a Real-Time Risk Prediction Model for In-Hospital Cardiac Arrest in Critically Ill Patients Using Deep Learning: Retrospective Study. *JMIR Med. Inform.* **2020**, *8*, e16349. [[CrossRef](#)]
36. Kuurman, W.; Bailey, B.; Koops, W.; Grossman, M. A model for failure of a chicken embryo to survive incubation. *Poult. Sci.* **2003**, *82*, 214–222. [[CrossRef](#)]
37. Gil-Pozo, A.; Astudillo-Rubio, D.; Álvaro Ferrando Cascales.; Inchingolo, F.; Hirata, R.; Sauro, S.; Delgado-Gaete, A. Effect of gastric acids on the mechanical properties of conventional and CAD/CAM resin composites—An in-vitro study. *J. Mech. Behav. Biomed. Mater.* **2024**, *155*, 106565. [[CrossRef](#)]
38. Meng, H.; Xu, Y. Pirfenidone-loaded liposomes for lung targeting: Preparation and in vitro/in vivo evaluation. *Drug Des. Dev. Ther.* **2015**, *2015*, 3369–3376. [[CrossRef](#)]
39. Falcinelli, S.D.; Kilpatrick, K.W.; Read, J.; Murtagh, R.; Allard, B.; Ghofrani, S.; Kirchherr, J.; James, K.S.; Stuelke, E.; Baker, C.; et al. Longitudinal Dynamics of Intact HIV Proviral DNA and Outgrowth Virus Frequencies in a Cohort of Individuals Receiving Antiretroviral Therapy. *J. Infect. Dis.* **2020**, *224*, 92–100. [[CrossRef](#)]
40. Verhulst, P.F. *Nouveaux Mémoires de l'Académie Royale des Sciences et Belles-Lettres de Bruxelles*; Nabu Press: Charleston, SC, USA, 1845; Volume 18, p. 8.
41. Bliss, C.I. The Method of Probits. *Science* **1934**, *79*, 38–39. [[CrossRef](#)]
42. Epremian, E.; Mehl, R.F. *Investigation of Statistical Nature of Fatigue Properties*; National Advisory Committee for Aeronautics: National Advisory Committee for Aeronautics: Washington, DC, USA, 1952.
43. Gompertz, B. On the nature of the function expressive of the law of human mortality, and on a new mode of determining the value of life contingencies. *Philos. Trans. R. Soc. Lond.* **1825**, *115*, 513–585. [[CrossRef](#)]
44. Winsor, C.P. The Gompertz Curve as a Growth Curve. *Proc. Natl. Acad. Sci. USA* **1932**, *18*, 1–8. [[CrossRef](#)]
45. von Bertalanffy, L. Untersuchungen Über die Gesetzlichkeit des Wachstums. I. Teil: Allgemeine Grundlagen der Theorie; Mathematische und physiologische Gesetzlichkeiten des Wachstums bei Wassertieren. *Wilhelm Roux Arch. Entwickl. Mech. Org.* **1934**, *131*, 613–652. [[CrossRef](#)]
46. Weibull, W. *The Statistical Theory of the Strength of Materials*. *Ingeniors Vetenskaps Academy Handlingar (151)*; Generalstabens Litografiska Anstalts Förlag: Stockholm, Sweden, 1939; pp. 1–45.
47. Rosin, P.; Rammler, E. The Laws Governing the Fineness of Powdered Coal. *J. Inst. Fuel* **1933**, *7*, 29–36.
48. Yada, S.; Hamada, C. Application of Bayesian hierarchical models for phase I/II clinical trials in oncology. *Pharm. Stat.* **2017**, *16*, 114–121. [[CrossRef](#)]
49. Fouarge, E.; Monseur, A.; Boulanger, B.; Annoussamy, M.; Seferian, A.M.; Lucia, S.D.; Lilien, C.; Thielemans, L.; Paradis, K.; Cowling, B.S.; et al. Hierarchical Bayesian modelling of disease progression to inform clinical trial design in centronuclear myopathy. *Orphanet J. Rare Dis.* **2021**, *16*, 3. [[CrossRef](#)]
50. Haber, L.T.; Reichard, J.F.; Henning, A.K.; Dawson, P.; Chinthrajah, R.S.; Sindher, S.B.; Long, A.; Vincent, M.J.; Nadeau, K.C.; Allen, B.C. Bayesian hierarchical evaluation of dose-response for peanut allergy in clinical trial screening. *Food Chem. Toxicol.* **2021**, *151*, 112125. [[CrossRef](#)]
51. Curigliano, G.; Gelderblom, H.; Mach, N.; Doi, T.; Tai, D.; Forde, P.M.; Sarantopoulos, J.; Bedard, P.L.; Lin, C.C.; Hodi, F.S.; et al. Phase I/Ib Clinical Trial of Sabatolimab, an Anti-TIM-3 Antibody, Alone and in Combination with Spartalizumab, an Anti-PD-1 Antibody, in Advanced Solid Tumors. *Clin. Cancer Res.* **2021**, *27*, 3620–3629. [[CrossRef](#)]
52. Gotuzzo, A.G.; Piles, M.; Della-Flora, R.P.; Germano, J.M.; Reis, J.S.; Tyska, D.U.; Dionello, N.J.L. Bayesian hierarchical model for comparison of different nonlinear function and genetic parameter estimates of meat quails. *Poult. Sci.* **2019**, *98*, 1601–1609. [[CrossRef](#)]

53. Paun, I.; Husmeier, D.; Hopcraft, J.G.C.; Masolele, M.M.; Torney, C.J. Inferring spatially varying animal movement characteristics using a hierarchical continuous-time velocity model. *Ecol. Lett.* **2022**, *25*, 2726–2738. [[CrossRef](#)]
54. Ramos, A.N.; Fenton, F.H.; Cherry, E.M. Bayesian inference for fitting cardiac models to experiments: estimating parameter distributions using Hamiltonian Monte Carlo and approximate Bayesian computation. *Med. Biol. Eng. Comput.* **2023**, *61*, 75–95. [[CrossRef](#)]
55. Yang, W.; Tempelman, R.J. A Bayesian antedependence model for whole genome prediction. *Genetics* **2012**, *190*, 1491–1501. [[CrossRef](#)]
56. Selle, M.L.; Steinsland, I.; Lindgren, F.; Brajkovic, V.; Cubric-Curik, V.; Gorjanc, G. Hierarchical Modelling of Haplotype Effects on a Phylogeny. *Front. Genet.* **2021**, *11*, 531218. [[CrossRef](#)]
57. Mukaddim, R.A.; Meshram, N.H.; Mitchell, C.C.; Varghese, T. Hierarchical Motion Estimation With Bayesian Regularization in Cardiac Elastography: Simulation and *Vivo* Validation. *IEEE Trans. Ultrason. Ferroelectr. Freq. Control* **2019**, *66*, 1708–1722. [[CrossRef](#)]
58. Andrews, L.C. *Special Functions of Mathematics for Engineers*, 2nd ed.; SPIE Press: Bellingham, WA, 1998; p. 110.
59. Muller, R. Sequence A007680 in the On-Line Encyclopedia of Integer Sequences (n.d.). Available online: <https://oeis.org/A007680> (accessed on 11 November 2024).
60. Abramowitz, M.; Stegun, I.A. *Handbook of Mathematical Functions with Formulas, Graphs, and Mathematical Tables*, 10th ed.; The Superintendent of Documents, U.S. Government Printing Office: Washington, DC, USA, 1972. Available online: <https://personal.math.ubc.ca/~cbm/aands/index.htm> (accessed on 9 November 2024).
61. Carlitz, L. The inverse of the error function. *Pac. J. Math.* **1963**, *13*, 459–470. [[CrossRef](#)]
62. Toda, H. An Optimal Rational Approximation for Normal deviates for Digital Computers. *Bull. Electrotech. Lab.* **1967**, *31*, 1259–1270.
63. Guennebaud, G.; Jacob, B.; Avery, P.; Bachrach, A.; Barthelemy, S.; Becker, C.; Benjamin, D.; Berger, C.; Blanco, J.L.; Borgerding, M.; et al. Eigen v3. 2010. Available online: <http://eigen.tuxfamily.org> (accessed on 11 November 2024).
64. Genz, A.; Bretz, F. *Computation of Multivariate Normal and t Probabilities*; Lecture Notes in Statistics; Springer: Heidelberg, Germany, 2009.
65. Harris, C.R.; Millman, K.J.; van der Walt, S.J.; Gommers, R.; Virtanen, P.; Cournapeau, D.; Wieser, E.; Taylor, J.; Berg, S.; Smith, N.J.; et al. Array programming with NumPy. *Nature* **2020**, *585*, 357–362. [[CrossRef](#)]
66. Weissmann, B. Multivariate-Normal (v0.1.2): A Pure-Javascript Port of NumPy's random.multivariate\_normal, for node.js and the Browser. 2023. Available online: <https://www.npmjs.com/package/multivariate-normal> (accessed on 12 November 2024).

**Disclaimer/Publisher's Note:** The statements, opinions and data contained in all publications are solely those of the individual author(s) and contributor(s) and not of MDPI and/or the editor(s). MDPI and/or the editor(s) disclaim responsibility for any injury to people or property resulting from any ideas, methods, instructions or products referred to in the content.